Applied Catalysis B: Environmental 186 (2016) 136–142

Contents lists available at ScienceDirect

Applied Catalysis B: Environmental

journal homepage: www.elsevier.com/locate/apcatb

# Residue-based iron catalyst for the degradation of textile dye via heterogeneous photo-Fenton

Fernando F. Dias[a,c], Aline A.S. Oliveira[b], Ana P. Arcanjo[a], Flávia C.C. Moura[b], José G.A. Pacheco[a,*]

[a] Department of Chemical Engineering, Universidade Federal de Pernambuco, 50740-521 Recife, PE, Brazil
[b] Departament of Chemistry, Universidade Federal de Minas Gerais, 31270-901 Belo Horizonte, MG, Brazil
[c] UAG, Universidade Federal Rural de Pernambuco, 55.292-270 Garanhuns, PE, Brazil

ARTICLE INFO

*Article history:*
Received 22 March 2015
Received in revised form
25 December 2015
Accepted 29 December 2015
Available online 3 January 2016

*Keywords:*
Heterogeneous catalysis
Residue-based catalyst
Red mud
Photo-Fenton
Textile dye

ABSTRACT

In this work, the use of a residue-based catalyst for heterogeneous photo-Fenton of Reactive black 5 (RB5) textile dye was evaluated. The catalyst was prepared by chemical vapor deposition of ethanol on a red mud residue, an important waste of the aluminum industry rich in iron oxide. The catalyst was characterized by different techniques, i.e., Mössbauer spectroscopy, Raman spectroscopy, CHN elemental analysis, BET surface area, and scanning and transmission electron microscopies. Results showed that the iron phases present in the red mud are reduced and a carbon coating is formed, protecting the catalyst from excessive iron leaching. The photo-Fenton experiments were carried out by varying pH, $H_2O_2$ concentration and radiation power and assessing dye conversion as the response variable. Studies on textile dye degradation showed that low pH favors the reaction and 100% photo-degradation efficiency was obtained, reducing the toxicity of the dye. The best operational condition was achieved at pH 3 and $H_2O_2$ initial concentration of 11 mM, after 60 min of reaction. Kinetic data related to RB5 dye degradation were well fitted to the Langmuir–Hinshelwood model in the range of 20–50 mg $L^{-1}$ of RB5 initial concentration with obtained initial rate constant of $9.4 \times 10^{-8}$ mol $L^{-1}$ $min^{-1}$. A reaction pathway was proposed in which the $H_2O_2$ is activated by surface $Fe^{2+}$ sites on RM based catalyst, especially in the presence of light, producing •OH radicals in a heterogeneous photo-Fenton-like mechanism to oxidize the organic pollutant Reactive black 5 dye.



## 1. Introduction

Red mud (RM) is a by-product of the Bayer process for alumina production. This process has been used for over 120 years and residues are primarily disposed of in long-term storage in a number of different forms [1]. Ideally, this residue could be used as an industrial by-product for other applications, leading to a zero waste situation. Despite over 50 years of research and hundreds of publications and patents on the subject, little evidence exists of any significant way that RM has been put to use [2].

Brazil has a large capacity for alumina production and 1.0–1.5 tons of RM are generated per ton of alumina produced. It is estimated that just in Brazil more than 20 Mt of red mud are generated every year without proper destination [3].

The main constituents of RM include $Fe_2O_3$, $Al_2O_3$, $SiO_2$, $TiO_2$, $Na_2O$, CaO and MgO, which are very interesting species for chemical applications. However, due to its high alkalinity RM is harmful to water, land and air, and demands much space for storage. It is expensive to contain and to build reservoirs to prevent RM spills into the environment. A worldwide effort has been made recently to find appropriate applications for RM residue [4], such as $CO_2$ capture [5,6], polymer and cements additives [7], heavy metals adsorption in contaminated soils [8,9] and contaminants adsorption from aqueous solution [10–12]. Moreover, the high iron content of RM motivates its use in catalytic applications [2,13–20], such as wastewater treatment. Brazil houses important industrial centers, including industries based on textile dye processing. The lack of treatment of wastewater from this industry, combined with high water scarcity, represents a serious environmental issue.

The textile industry produces large amounts of effluents contaminated with dyes, which are toxic to humans and environment. Textile dyes are generally recalcitrant compounds with high molecular weight. These dyes are highly resistant to microbiological

* Corresponding author.
*E-mail addresses:* jose.pacheco@ufpe.br, geraldo.ufpe@gmail.com (J.G.A. Pacheco).

http://dx.doi.org/10.1016/j.apcatb.2015.12.049
0926-3373/

degradation and may not be degraded readily by biological treatment methods [21]. Adsorption processes have been widely used to remove these pollutants from wastewater but these processes merely transfer them from an aqueous to a solid phase, which does not solve the problem. Given this, advanced oxidation processes (AOPs) have been studied in the recent years as a technique for the degradation of pollutants in wastewater treatment [22,23].

AOPs are based on the generation of •OH radicals, powerful reactive species, capable of oxidizing a wide range of organic compounds [23–25]. Homogeneous photo-Fenton is a common AOP, in which soluble iron II is the catalyst; but the difficulty of catalyst recovery is a process drawback [26]. Thus, efforts have been made to find efficient heterogeneous iron catalysts such as Fe-clays [27], $Fe/TiO_2$ [28] and $Fe_3O_4/\gamma\text{-}Al_2O_3$ [29]. A number of heterogeneous photo-Fenton studies have identified the optimized operational variables, e.g., the pH (from 2.8 to 7.0), $H_2O_2$ concentration (from 0.1 to 5.0 mmol $L^{-1}$) and concentration of solid catalyst (from 0.1 to 5.0 g $L^{-1}$) [17–20]. Zero-valent iron ($Fe^0$) has been also studied as a solid catalyst in the so called photo-Fenton-like reaction [30]. In this process, the Fe° is converted into ferrous ion ($Fe^{2+}$) that acts as a catalyst for the Fenton reaction to produce •OH [31].

Few studies have been reported on the application of RM as catalyst for AOPs. Saputra et al. [32] used red mud supported Co catalysts for phenol degradation in aqueous phase. Oliveira et al. [33,34] and Costa et al. [35] studied modified red mud for degradation of dyes, thiophene, quinoline and dibenzothiophene.

A concern about the heterogeneous photo-Fenton process is that attention has been focused on the photo-degradation of toxic compounds under UV irradiation. The use of artificial ultraviolet lamps for degrading industrial effluents consumes a large amount of expensive electrical energy. It is known that the sunlight that reaches the Earth surface contains only about 4% of UV radiation spectra [36]. Therefore, it is desirable to find heterogeneous photo-Fenton catalysts based on sunlight irradiation instead of an artificial UV light source, particularly in Brazil, where there is high availability of sun irradiation throughout the year.

In this contribution, we have studied the degradation of Reactive black 5 (RB5) textile dye using a magnetic carbon coated catalyst based on red mud residue and simulated sunlight irradiation by heterogeneous Fenton and photo-Fenton processes.

## 2. Experimental

### 2.1. Preparation and characterization of the catalyst

The catalyst RM/C was prepared by chemical vapor deposition (CVD) reaction. RM was previously washed with deionized water to reduce its alkalinity and was dried at 60 °C over 24 h. After drying, the RM (50 mg) was heated at a rate of 5 °C $min^{-1}$ up to 700 °C in an horizontal furnace (Lindberg Blue) with ethanol (Vetec 99.5%, Brazil) as the carbon source at ca. 6% in $N_2$ (30 mL $min^{-1}$) and maintained at this temperature for 3 h. After this time, the system was cooled down to room temperature under ethanol/$N_2$ flow. The produced material, RM/C, was characterized by Mössbauer spectroscopy (room temperature in a spectrophotometer CMTE MA250, with constant acceleration, Co source, Rh matrix and α-Fe as reference), Raman spectroscopy (Bruker SENTERRA, helium–neon laser at wavelength 633 nm), scanning electron microscopy – SEM (microscope SEG – Quanta 200–SEI) and transmission electron microscopy – TEM (microscope Tecnai G2 200 kV – SEI). In order to obtain the values of band gap, the catalyst was analyzed by diffuse reflectance. The diffuse reflectance spectra were obtained using a Varian Cary 5 instrument equipped with diffuse reflectance accessory.

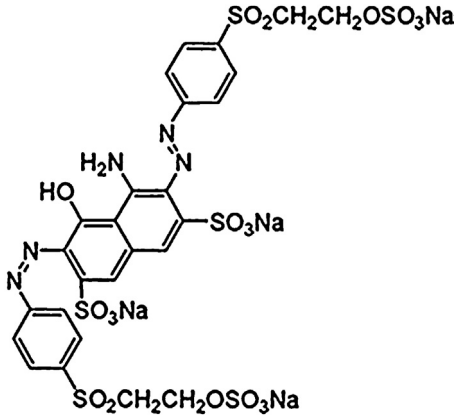


**Fig. 1.** Structure of the Reactive black 5 (RB5) textile dye.

### 2.2. Degradation of Reactive Black 5 textile dye

Hydrogen peroxide ($H_2O_2$ 30%, Vetec) and a commercial textile dye RB5 (Hangzhou Color Rich Chem Co., China), Fig. 1, were used as reagents and $H_2SO_4$ (98%, Vetec) and NaOH (99%, Vetec) were used for pH adjustment. The degradation of the dye was performed with a $2^2$ factorial experimental plan using as independent variables the initial concentration of hydrogen peroxide (11 mM, 22 mM, 33 mM) and pH (3, 6 and 9). The influence of $H_2O_2$ concentration was studied in the range of 11–97 mM $H_2O_2$, at pH 3. The degradation of the RB5 dye was used as the dependent variable. A catalyst concentration (RM/C) of 0.5 g $L^{-1}$ and a dye concentration of 50 mg $L^{-1}$ were held constant. The dye concentration was measured over time by UV–vis analysis in a Biochrom Libra S12 spectrophotometer using the peak of higher absorption at 595 nm. A batch reactor with 300 mL solution under stirring of 450 rpm was used. The lamp used in the tests was a SunLight Osran 300 W lamp, which has a light spectrum similar to sunlight. The radiation in the system was measured with a radiometer UVA/UVB MRU-201 in the range between 8.5 and 36 W $m^{-2}$. The RB5 solution (50 mg $L^{-1}$) was stirred in the dark for 30 min before reaction under light and $H_2O_2$ addition.

### 2.3. Toxicity

The toxicity analysis of the degraded dye was performed according to the method reported by Mamindy-Pajany et al. [37]. This method uses photosynthetic enzyme complexes (PECs) and stabilized aqueous photosynthetic system (SAPS) in a LuminoTox-Lab Bell analyzer. Photosynthetic activity is based on the fluorescence production. The fluorescence photosynthetic efficiency (quantum yield $\Phi$) is measured when the PECs/SAPS are unexposed ($\Phi_{zero}$) or exposed ($\Phi_{SAMPLE}$) to different concentrations of a toxic compound. 2.0 mL of pure deionized water or samples of RB5 solutions after reaction and neutralization were added to a cuvette at room temperature (25 °C), followed by the addition of 100 μL of PECs/SAPS, gentle mixing and resting for 15 min in the dark before reading the photoluminescence in the LuminoTox analyzer. The inhibition is calculated as follows: Inhibition $(\%) = [(\Phi_{zero} - \Phi_{SAMPLE})/(\Phi_{zero})] \times 100$.

## 3. Results and discussion

### 3.1. Characterization of the catalyst

The RM/C catalyst was produced by a chemical vapor deposition (CVD) process of RM residue and ethanol at 700 °C. Characterization results show that during the CVD process ethanol reacts with RM to

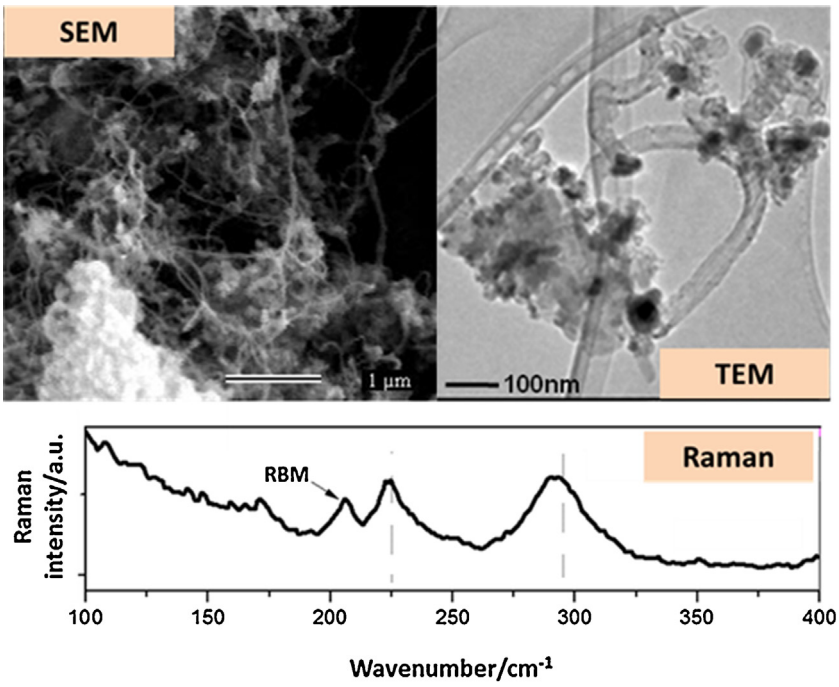


**Fig. 2.** SEM and TEM images and Raman spectrum obtained of the red mud catalyst after CVD process with ethanol (RM/C).

**Table 1**
Mössbauer hyperfine parameters determined for pure RM and RM/C catalyst.

| Sample | Phase | δ/mm s$^{-1}$ (0.05) | ε, Δ/mm s$^{-1}$ (0.05) | $B_{hf}/T$ (0.05) | RA/% (1) |
|---|---|---|---|---|---|
| Pure | α-$Fe_2O_3$ | 0.36 | −0.21 | 51.4 | 52 |
| RM | $Fe^{3+}$ | 0.36 | 0.58 | – | 48 |
| RM/C | α-$Fe_2O_3$ | 0.33 | 0.01 | 49.8 | 31 |
| | [$Fe_3O_4$] | 0.66 | 0.01 | 46.3 | 28 |
| | {$Fe_3O_4$} | 0.30 | 0.02 | 49.8 | 15 |
| | $Fe^{\circ}$ | 0.00 | 0.00 | 33.0 | 14 |
| | $Fe^{3+}$ | 0.67 | 1.97 | – | 12 |

δ—isomeric shift relative to α-Fe; ε—quadrupole shift; Δ—quadrupole splitting; $B_{hf}$ — hyperfine magnetic field; RA—relative subspectral area, []—tetrahedral site; {}—octahedral site.

produce a catalyst with reduced iron phases and carbon deposited on the surface [38]. The iron composition of the catalyst RM/C was studied by Mössbauer spectroscopy. The hyperfine parameters generated from the Mössbauer spectrum (Fig. S1, Supplementary material) are shown in Table 1.

Pure RM (before CVD process) contains only $Fe^{3+}$ species, i.e., α-$Fe_2O_3$ and dispersed $Fe^{3+}$, which are reduced during the CVD process to $Fe_3O_4$ and $Fe^0$. These reduced phases provide the main active species for the photo-Fenton reactions (see Section 3.4), and are responsible for the magnetic behavior of the catalyst.

Carbon partially coats the RM preventing iron oxidation and excessive leaching. CHN elemental analysis showed that RM/C contained 15% carbon.

The surface area of the catalyst was obtained by $N_2$ adsorption using the BET method. RM/C has a specific surface area of 68 m$^2$ g$^{-1}$ while pure RM has 24 m$^2$ g$^{-1}$. Pure RM presents mainly macropores with diameters larger than 50 nm, which explains its low specific surface area. On the other hand, the RM/C catalyst exhibits more micro and mesopores smaller than 10 nm, which is likely responsible for its higher surface area [38]. The increase in the surface area can be attributed to the large area of the carbon in different forms such as nanotubes and nanofilaments grown on the RM surface and their entangled arrangement. These carbon structures can be confirmed by Raman spectroscopy (Fig. 2). The Raman spectra obtained show an intense G band, related to organized carbon structures. SEM and TEM images (Fig. 2) show that the RM/C material presents irregular grains with a wide size particles distribution. Nanometric Fe particles, from 10 to 100 nm in diameter, can be seen inside the carbon filaments. The complete characterization of these materials has been reported by Oliveira et al. [38].

### 3.2. Degradation of Reactive Black 5 textile dye by photo-Fenton reaction

The dye degradation was expressed as $C_t/C_o$ where $C_t$ and $C_o$ are instantaneous and initial concentrations of RB5, respectively. The efficiency of degradation $[1-(C_t/C_o)]\times 100$ was monitored over time.

#### 3.2.1. Influence of radiation power in the heterogeneous photo-Fenton process

The catalyst was first left in contact with RB5 dye in the dark to evaluate the adsorption process. Fig. S3 (Supplementary material) shows that between 10 and 22% of the dye is adsorbed over 90 min. Previous works have shown that this catalyst adsorbs less than 5% of different organic substrates, i.e., lipophilic dye Sudan IV, thiophene, dibenzothiophene and quinoline (60 min of contact, 4 g L$^{-1}$ catalyst and pH 6) [26]. Adsorption capacities vary with the type of organic species, as well as the pH and catalyst composition. Organic carbon presented on the surface of RM may favor adsorption by interacting with the organic structure of the textile dye.

The effect of radiation power on the photo-Fenton system (RM/C/$H_2O_2$/UV) using 11 mM $H_2O_2$ and pH 3 is shown in Fig. 3.

Results show that a higher activity in the heterogeneous photo-Fenton is achieved with higher power radiation, i.e., 100% of concentration decay at 36 W m$^{-2}$ and 20% at 8.5 W m$^{-2}$. Boyjoo et al. [39] carried out a study of the light intensity distribution in photocatalytic reactors showing that the effect of the lamp power on the system depends on the absorption coefficient of the catalyst, catalyst concentration and the distance from the light source. The radiation increases system activity favoring the formation of

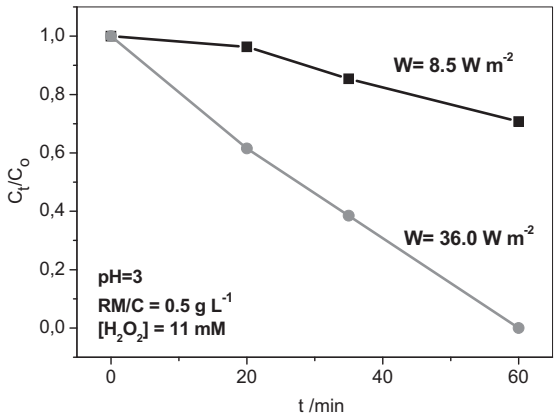


**Fig. 3.** Influence of radiation power on the degradation of RB5 dye (50 mg $L^{-1}$) by photo-Fenton using RM/C (0.5 g $L^{-1}$)/$H_2O_2$/UV and radiation of 8.5–36 W $m^{-2}$, pH 3 and $H_2O_2$ concentration = 11 mM.

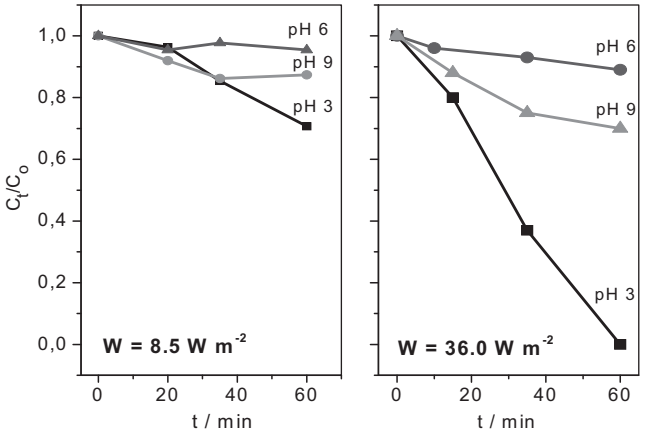


**Fig. 4.** Degradation of RB5 dye (50 mg $L^{-1}$) by photo-Fenton at different pH values using radiation power 8.5 or 36 W $m^{-2}$ (catalyst concentration RM/C = 0.5 g $L^{-1}$, [$H_2O_2$] = 11 mM, pH = 3, 6 and 9, reaction time 60 min).

radicals, producing a highly oxidizing species as shown in the following equations (Eqs. (1)–(3) [40]:

$$H_2O + h\nu \rightarrow {}^{\bullet}H + {}^{\bullet}OH \quad (1)$$

$$H_2O_2 + h\nu \rightarrow 2{}^{\bullet}OH \quad (2)$$

$$R + h\nu \rightarrow R^{\bullet} \quad (3)$$

Radiation may also enhance the heterogeneous Fenton activity on the surface of the iron particles, by promoting the photoreduction of $-Fe^{3+}OH$ to $-Fe^{2+}$, which subsequently reacts with $H_2O_2$ generating •OH radicals on the surface of the iron particles (Eqs. (4)–(5) [40].

$$Fe^{3+}OH_{(surf)} + h\nu \rightarrow Fe^{2+}{}_{(surf)} + {}^{\bullet}OH \quad (4)$$

$$Fe^{2+}{}_{(surf)} + H_2O_2 \rightarrow Fe^{3+}{}_{(surf)} + OH^- + {}^{\bullet}OH \quad (5)$$

*3.2.2. Influence of pH in the heterogeneous photo-Fenton process*

The influence of pH in the heterogeneous photo-Fenton oxidation of RB5 dye in the presence of RM/C catalyst was evaluated. Fig. 4 shows the decrease of dye concentration over time and degradation efficiency using a radiation power of 8.5 and 36 W $m^{-2}$.

100% of dye degradation was obtained at a radiation power of 36 W $m^{-2}$ and pH 3, compared to 30 and 40% of degradation efficiency using the same radiation power and pH 6 and 9, respectively. The degradation of RB5 using radiation power of 8.5 W $m^{-2}$ showed lower efficiency for all pH studied, i.e., 20, 30, and 42% at pH 6, 9, and 3, respectively.

Previous experiments have demonstrated that low pH favors photo degradation. Vinita et al. [41] reported that pH strongly interferes in the formation of hydroxyl radicals and in the oxidation of organic substrates. An acidic medium (low pH) enhances radical formation and organic compound oxidation. At pH 3 the formation of $Fe(OH)^{2+}$, the most photo-active $Fe^{3+}$-hydroxyl complex, is favored under UV-A and visible solar light species [42,43]. Leaching tests were performed in the solutions after reaction and soluble iron species were negligible, reaching no more than 1–4% of the total iron content. This concentration of iron cannot be responsible for the high degradation activity of RB5 observed.

Carbon present in the material is essential to hold iron on the surface of the solid during the reaction [41]. Moreover, carbon can also enhance the degradation of the organic dye by surface oxygenated groups, such as phenolic, and carboxylic groups, besides favoring the initial adsorption of the organic dye that enhances the oxidation process.

*3.2.3. Influence of $H_2O_2$ concentration in the heterogeneous photo-Fenton process*

Fig. 5a shows the influence of $H_2O_2$ concentration at different pH values on the efficiency of dye degradation with heterogeneous photo-Fenton process RM/C/$H_2O_2$/UV, based on experimental design $2^2$. The calculated effects of $H_2O_2$ and pH are shown in Table S1 (Supplementary material). Results show that only pH was statistically significant with 95% confidence in the ranges for $H_2O_2$ (11, 22 and 33 mM) and pH (3, 6 and 9). The influence of the $H_2O_2$ concentration at pH 9 is very small; however at pH 3, it is significant (Fig. 5a). The best efficiency is obtained with 11 mM of $H_2O_2$ at pH 3, leading to complete dye degradation.

With the aim of observing the system behavior over a wide range of $H_2O_2$ concentrations, experiments were performed up to 97 mM of $H_2O_2$. Fig. 5(b) shows the results of RB5 degradation experiments with different concentrations of $H_2O_2$, using a pH 3 and a radiation power of 36 W $m^{-2}$. Low pH favors RB5 degradation as observed above and the influence of $H_2O_2$ concentration in the ranges studied (6 up to 97 mM $H_2O_2$) is significant at this pH. Similar behavior was observed in Fenton-like systems (H–Fe–S) by Gao et al. [44].

The production of •OH from $H_2O_2$ is the key step of the Fenton process. The influence of $H_2O_2$ on the system can be explained by the fact that at low concentrations, a small amount of •OH radicals is formed, reducing the efficiency of dye degradation. At high $H_2O_2$ concentrations, the efficiency also decreases due to excess of •OH generated at the beginning of the process, which may lead to undesirable parallel reactions that form $H_2O$ and $O_2$ [45–48]. In addition, due to the high amount of $H_2O_2$ the •OH radicals are consumed to produce hydroperoxyl radicals (•OOH) (Eq. (6)), which presents a lower reduction potential ($E^\circ$ = 1.42 V) compared to the •OH radical ($E^\circ$ = 2.80 V) having a negative effect on the process [45–48].

After the initial experimental design, experiments over a wide range of $H_2O_2$ concentrations were performed in order to test the limits, i.e., to verify in which $H_2O_2$ concentration undesirable parallel reactions would be favored, decreasing the degradation efficiency. According to the literature, this concentration would be higher than 83 mM [49].

The best activity was achieved with 11 mM of $H_2O_2$, in the reaction conditions studied. At higher $H_2O_2$ concentrations e.g., 33 and 65 mM the activity decreases similarly (Fig. 5b). On the other hand, when $H_2O_2$ concentration is increased to a very high concentration i.e., 97 mM, we observe that the activity clearly decreases, confirming that undesirable parallel reactions are favored at higher $H_2O_2$ concentrations.

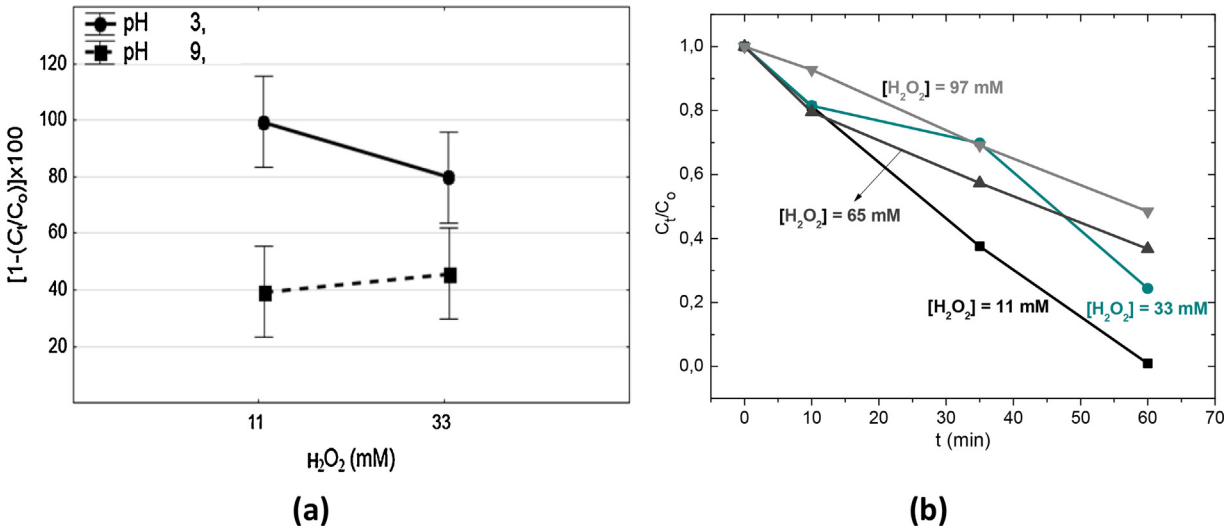


**Fig. 5.** Influence of $H_2O_2$ concentration on the degradation of RB5 dye (50 mg $L^{-1}$) on RM/C catalyst (0.5 g $L^{-1}$): (a) At different pH values. (b) Over time at pH 3 (radiation power 36 W $m^{-2}$).

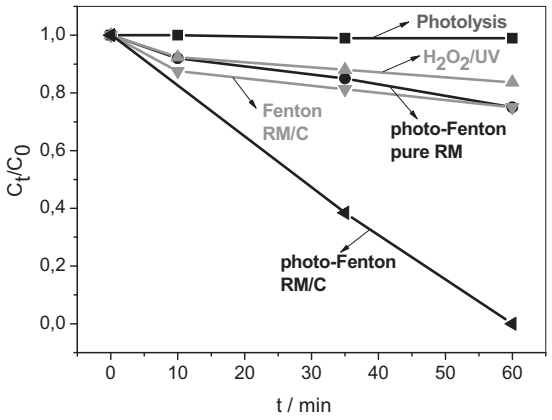


**Fig. 6.** Degradation of RB5 dye (50 mg $L^{-1}$) by different process: UV (photolysis), $H_2O_2$/UV, heterogeneous Fenton on RM/C, heterogeneous photo-Fenton on pure RM and on RM/C. Catalyst concentration = 0.5 g $L^{-1}$, [$H_2O_2$] = 11 mM.

### 3.2.4. Heterogeneous photo-Fenton comparing to other processes

To access the influence of the catalyst, peroxide, and the presence of radiation on RB5 degradation, experiments were carried out under different conditions: (i) using RM/C/$H_2O_2$ without radiation (Fenton) and after light irradiation (photo-Fenton), (ii) using only $H_2O_2$ without a catalyst ($H_2O_2$ photolysis), (iii) using only light (photolysis of RB5), and (iv) pure red mud RM/$H_2O_2$/UV—Fig. 6.

The photolysis of RB5 (blank) using a SunLight lamp with a radiation power of 36 W $m^{-2}$ showed no activity and degraded only 1% of the dye, while with the use of $H_2O_2$ after irradiation without catalyst ($H_2O_2$ 11 mM) 16% of the dye was degraded. The increased activity of the light irradiation experiment in the presence of $H_2O_2$ can be explained by the formation of radicals, as shown above in (Eqs. (1)–(3)).

The use of pure red mud as catalyst with $H_2O_2$/UV (heterogeneous photo-Fenton) degraded only 25% of the dye. The RM/C catalyst without radiation (heterogeneous Fenton) also led to 25% of degradation. The best result was reached via heterogeneous photo-Fenton using RM/C/$H_2O_2$/UV, with 100% of dye reduction. The degradation efficiency of RB5 followed this order: RM/C/$H_2O_2$/UV (heterogeneous photo-Fenton) > RM/C/$H_2O_2$ (heterogeneous Fenton) ≈ RM/$H_2O_2$/UV > $H_2O_2$/UV > UV (photolysis).

The process using only the SunLight lamp (photolysis of RB5) was not efficient. On the other hand, the presence of the catalyst combined with the UV light was very important for the RB5 degradation. The band gap energy of the catalyst was determined by experiments of diffuse reflectance as 4.58 eV (Fig. S2, Supplementary material), which means that this catalyst can be activated only by the UV light from the SunLight lamp. Sunlight itself, however, is composed of only 3–5% of ultra-violet radiation and about 45–50% of visible light.

### 3.2.5. Kinetics of the heterogeneous photo-Fenton process

The literature reports studies on the initial rate Langmuir–Hinshelwood (L–H) kinetics for organic compound degradation with adsorption/desorption equilibrium under either light or dark conditions [50,51]. The L–H model is represented by $r_o = k_{LH} \times K_L \times C_o/[1+K_L \times C_o]$, where $r_o$ is the initial reaction rate, obtained by the variation of the initial concentration of the substrate ($C_o$), $k_{LH}$ is the apparent constant rate and $K_L$ is the equilibrium constant for adsorption/desorption, which is independent of the photon flux. The L–H model parameters in our study were estimated from the linearized curve $1/r_o$ vs $1/C_o$ obtaining the adsorption rate constant values $k_{LH} = 9.4 \times 10^{-8}$ mol $L^{-1}$ $min^{-1}$ and $K_L = 3.1 \times 10^4$ L $mol^{-1}$ for the experimental conditions used (Fig. 7). Adsorption is an important step of the oxidation reaction and the higher the adsorption rate constant values the higher is the oxidant rate constant [51]. Similar kinect studies may be found in the literature for the degradation of RB5 dye on $TiO_2$ [52].

### 3.3. Toxicity

Fig. 8 shows the toxicity inhibition curve of the Reactive Black 5 before and after degradation at different reaction times using the best operational condition, i.e., pH 3 and 11 mM of $H_2O_2$. Initially (time zero), the aqueous solution of RB5 50 ppm promotes 42% of inhibition, which increases to 47% after 20 min of photo-Fenton reaction treatment. After 60 min reaction, the inhibition decreases to 24% and to 22% after 120 min. The increase in toxicity in the first 20 min of reaction can be explained by the production of intermediate products, which are more toxic than the original RB5 dye, similar to results reported by Karci [53]. This toxicity is based on the fluorescence activity of photosynthetic enzyme complexes (PECs) extracted from plant cells and stabilized aqueous photosynthetic systems (SAPs) obtained from *Chlorella vulgaris*.

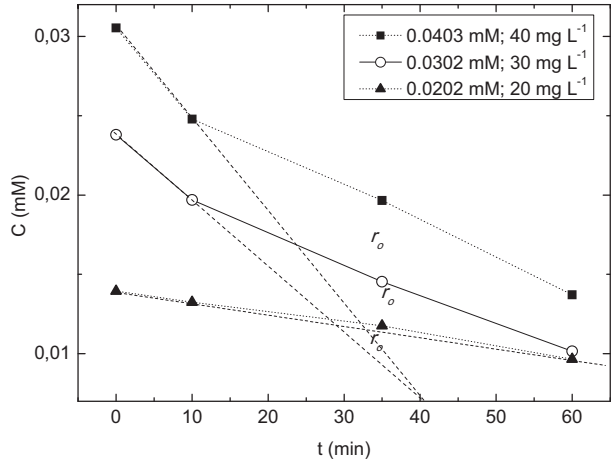


**Fig. 7.** Kinetic curve for the degradation of RB5 dye by photo-Fenton using RM/C (0.5 g $L^{-1}$)/$H_2O_2$/UV, $H_2O_2$ initial concentration = 11 mM and pH 3 in different concentrations of RB5 (20, 30 and 40 mg $L^{-1}$).

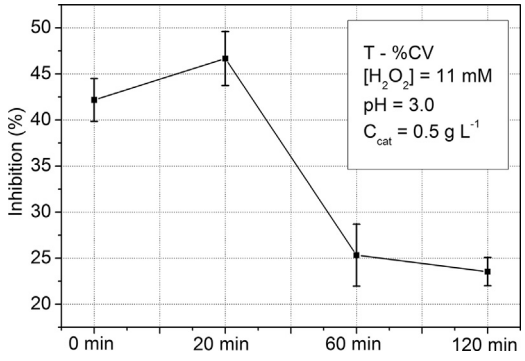


**Fig. 8.** Inhibition curve of the RB5 before and after degradation in different reaction times, in the optimal condition of pH 3 and concentration of $H_2O_2$ = 11 mM.

PECs are membranes isolated from chloroplasts, which emit fluorescence when stimulated by radiation. When toxic compounds are present in water, the photosynthetic electron chain reaction is inhibited, decreasing the fluorescence of PECs. This method is useful for measuring the global fitotoxicity and ecotoxicity of degraded toxic compounds [54].

Konstantinou and Albanis [52] reported that the primary by-products from the photocatalytic degradation of azo dyes come from the breaking of the bonds around the azo group, producing different acids, quinones and naphthalene derivatives, such as sulfanilic acid, benzenesulfonic acid, hydroxybenzenesulfonic acid, 2-naphthol, dihydroxynaphthalene and hydroxy-1,4-naphthoquinone. Among these compounds, the most toxic is naphthoquinone, which has a LD50(rat) of 190 mg/kg [55] and may contribute to an increase in the global toxicity of the degraded dye in the first steps of the oxidation process. A recent study conducted by Vasconcelos et al. [56] shows that the degradation route of RB5 dye involves an initial cleavage of the azo bond. The intermediates/by-products of RB5 degradation identified by this group include phenol, aliphatic acids and $CO_2$ and $H_2O$ in case of complete mineralization of the dye in the presence of •OH.

### 3.4. Reaction pathway of the production of hydroxyl radicals on the iron RM-based catalyst

Based on the characterization results shown above, pure RM contains only $Fe^{3+}$ phases, i.e., hematite ($\alpha$-$Fe_2O_3$) and dispersed $Fe^{3+}$, which are less active for $H_2O_2$ activation by the Fenton process. Moreover, experiments show that pure RM leachates iron species into aqueous phase. On the other hand, the RM/C catalyst has $Fe_3O_4$ that contains $Fe^{2+}$ species on the surface that are essential for its intense activity in the degradation reaction. Studies from the literature have shown that $Fe^{2+}_{surf}$ initiate the reaction by the generation of OH hydroxyl radicals from $H_2O_2$ via a Haber–Weiss mechanism [31,57–61] (Eq. (5)).

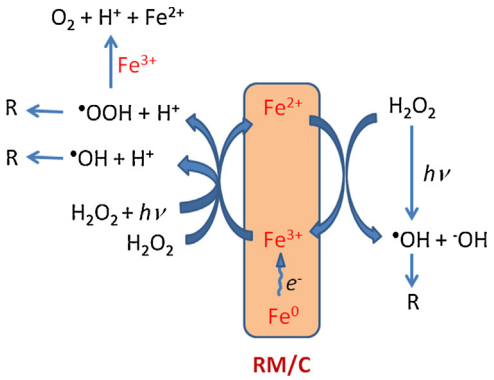


**Fig. 9.** Schematic pathway for hydroxyl radical production and oxidation of the pollutant organic material (R) on iron-red mud-based catalyst at pH 3.0.

The activity observed in the presence of RM/C and $H_2O_2$ in the Fenton process (without light) may be attributed to the heterogeneous Fenton reaction ($Fe^{2+}/H_2O_2$) catalyzed by $Fe^{2+}$ of the magnetite phase ($Fe_3O_4$) on the surface, as determined by Mössbauer spectroscopy results (Eq. (5)). The •OH radical may react with another $H_2O_2$ molecule to form •OOH (Eq. (6)) and OH transfers one electron to $Fe^{3+}$ regenerating the $Fe^{2+}$ species (Eq. (7)).

$$Fe^{2+}_{(surf)} + H_2O_2 \rightarrow Fe^{3+}_{(surf)} + OH^- + {}^{\bullet}OH \quad (5)$$

$$^{\bullet}OH + H_2O_2 \rightarrow {}^{\bullet}OOH + H_2O \quad (6)$$

$$^{\bullet}OOH + Fe^{3+}_{(surf)} \rightarrow Fe^{2+}_{(surf)} + H^+ + O_2 \quad (7)$$

In addition, the presence of $Fe^{3+}$ as $Fe_2O_3$ and dispersed $Fe^{3+}$ may also contribute to the reaction with $H_2O_2$. The $Fe^{2+}$ species can be regenerated through the reaction of $H_2O_2$ with $Fe^{3+}$ sites available on the surface of the particles leading also to the formation of •OOH (Eq. (8)). Consequently, new $Fe^{2+}$ sites are then formed, which may react with $H_2O_2$ to produce •OH radicals and the $Fe^{3+}$ sites are recovered through oxidation of $Fe^{2+}$ in a cyclic mechanism. This $Fe^{2+}$ regeneration, the rate determinant step of the Fenton process also occurs via $Fe^{3+}$ reduction in a photo-Fenton reaction (Eq. (9)).

$$Fe^{3+}_{(surf)} + H_2O_2 \rightarrow Fe^{2+}_{(surf)} + H^+ + HOO^{\bullet} \quad (8)$$

$$Fe^{3+}_{(surf)} + H_2O_2 + h\nu \rightarrow Fe^{2+}_{(surf)} + H^+ + {}^{\bullet}OH \quad (9)$$

Furthermore, the combination of Fe° with $Fe_3O_4$ improves the electron transfer from $Fe_3O_4$ to $H_2O_2$/•OH conversion by the Haber–Weiss reaction. The combination of $Fe^0$ and $Fe_3O_4$ creates an interface metal-oxide and the possibility of electron transfer from $Fe^0$ to the oxide. The interface metal-semiconductor is known to form an ohmic junction with very low resistance [61,62]. Zhou et al. [30] studied the degradation of the 4-chlorophenol kinetic process on the $Fe^0/H_2O_2$ catalyst, which occurs in two steps. In the first and slow step, the zero valent iron on the surface produces $Fe^{2+}$. In the second and fast step, $Fe^{2+}$ catalyzes the generation of •OH via the Fenton mechanism. Based on this and other mechanisms reported in the literature [30,31,63–66] we proposed a reaction pathway for hydroxyl radical production and oxidation of the dye (R), as shown in Fig. 9.

In this pathway, the $H_2O_2$ is activated by surface $Fe^{2+}$ sites on RM based catalyst that are oxidized to $Fe^{3+}$ to simultaneously pro-

duce •OH radicals via a heterogeneous Fenton-like mechanism. The dye (R) is sequentially oxidized by •OH radicals to produce oxidized species. In subsequent reactions, highly oxidizing •OOH are generated from •OH and $H_2O_2$ that are capable of oxidizing the organic compounds and furthermore regenerate $Fe^{2+}$ species from $Fe^{3+}$. $Fe^{2+}$ species may also be generated in the presence of the radiation or due to the electron transfer from $Fe^0$.

## 4. Conclusions

In this research, a promising material based on iron residue partially coated by carbon was obtained, RM/C. This material was produced from red mud waste and ethanol via chemical vapor deposition process. RM/C was applied in the heterogeneous photo-Fenton process for the degradation of the Reactive black 5 textile dye. The produced material shows irregular grains with particles size in a wide distribution, including nanometric Fe particles inside of carbon filaments that varied from 10 to 100 nm in diameter. RM/C had a specific surface area of 68 $m^2\ g^{-1}$ and interesting magnetic behavior. Besides being produced from a worthless and dangerous residue, the RM based catalyst reached 100% efficiency in the dye degradation after 60 min of photo-Fenton reaction at pH 3 and 11 mM of $H_2O_2$. Thus, the simplicity and low cost of using RM based catalyst and solar light in a photo-Fenton heterogeneous process may be a very promising technology for the removal of organic contaminants from wastewater.

## Acknowledgements

The authors would like to acknowledge the National Institute of Science and Technology for Environmental Studies (CNPq/INCT-EMA), FAPEMIG and project CAPES/PROCAD (88881.068433/2014-01) for financial support.

## Appendix A. Supplementary data

Supplementary data associated with this article can be found, in the online version, at http://dx.doi.org/10.1016/j.apcatb.2015.12.049.

## References

[1] E. Karimi, I.F. Teixeira, A. Gomez, E. de Resende, C. Gissane, J. Leitch, V. Jollet, I. Aigner, F. Berruti, C. Briens, P. Fransham, B. Hoff, N. Schrier, R.M. Lago, S.W. Kycia, R. Heck, M. Schlaf, Appl. Catal. B: Environ. 145 (2014) 187–196.
[2] C. Klauber, M. Grafe, G. Power, Hydrometallurgy 108 (2011) 11–32.
[3] A.A.S. Oliveira, I.F. Teixeira, L.P. Ribeiro, J.C. Tristao, A. Dias, R.M. Lago, J. Braz. Chem. Soc. 21 (2010) 2184–2188.
[4] S. Samal, A.K. Ray, A. Bandopadhyay, Int. J. Miner. Process. 118 (2013) 43–55.
[5] P. Renforth, W.M. Mayes, A.P. Jarvis, I.T. Burke, D.A.C. Manning, K. Gruiz, Sci. Total Environ. 421–422 (2012) 253–259.
[6] C. Si, Y. Ma, C. Lin, J. Hazard. Mater. 244–245 (2013) 54–59.
[7] W. Hajjaji, S. Andrejkovicova, C. Zanelli, M. Alshaaer, M. Dondi, J.A. Labrincha, F. Rocha, Mater. Des. 52 (2013) 648–654.
[8] W. Friesl-Hanl, K. Platzer, O. Horak, M.H. Gerzabek, Environ. Geochem. Health 31 (2009) 581–594.
[9] Y.Z. Huang, X.W. Hao, Chem. Ecol. 28 (2012) 37–48.
[10] V.L. Vukasinovic-Pesic, V.N. Rajakovic-Ognjanovic, N.Z. Blagojevic, V.V. Grudic, B.M. Jovanovic, L.V. Rajakovic, Chem. Eng. Commun. 199 (2012) 849–864.
[11] E. Kalkan, H. Nadaroglu, N. Dikbaş, E. Taşgın, N. Çelebi, Pol. J. Environ. Stud. 22 (2013) 417–429.
[12] V.V. Grudić, Đ. Perić, N.Z. Blagojević, V.L. Vukašinović-Pešić, S. Brašanac, B. Mugoša, Pol. J. Environ. Stud. 22 (2013) 377–385.
[13] K. Pirkanniemi, M. Sillanpaa, Chemosphere 48 (2002) 1047–1060.
[14] S. Ordonez, F.V. Diez, H. Sastre, Catal. Today 73 (2002) 325–331.
[15] S.B. Wang, H.M. Ang, M.O. Tade, Chemosphere 72 (2008) 1621–1635.
[16] A. Eamsiri, W.R. Jackson, K.C. Pratt, V. Christov, M. Marshall, Fuel 71 (1992) 449–453.
[17] J. Halasz, M. Hodos, I. Hannus, G. Tasi, I. Kiricsi, Colloid Surf. A 265 (2005) 171–177.
[18] J. Yanik, M.A. Uddin, K. Ikeuchi, Y. Sakata, Polym. Degrad. Stab. 73 (2001) 335–346.
[19] A. Lopez-Urionabarrenechea, I. de Marco, B.M. Caballero, M.F. Laresgoiti, A. Adrados, A. Aranzabal, Appl. Catal. B: Environ. 104 (2011) 211–219.
[20] J.F. Lamonier, F. Wyralski, G. Leclercq, A. Aboukais, Can. J. Chem. Eng. 83 (2005) 737–741.
[21] H. Kusic, N. Koprivanac, S. Horvat, S. Bakija, A.L. Bozic, Chem. Eng. J. 155 (2009) 144–154.
[22] N. Borràs, C. Arias, R. Oliver, E. Brillas, J. Electroanal. Chem. 689 (2013) 158–167.
[23] W.R.P. Barros, J.R. Steter, M.R.V. Lanza, A.C. Tavares, Appl. Catal. B: Environ. 180 (2016) 434–441.
[24] J.Y.T. Chan, S.Y. Ang, E.Y. Ye, M. Sullivan, J. Zhang, M. Lin, Phys. Chem. Chem. Phys. 17 (2015) 25333–25341.
[25] G.B. Ortiz de la Plata, O.M. Alfano, A.E. Cassano, Appl. Catal. B: Environ. 95 (2010) 14–25.
[26] A.S. Martins, V.M. Vasconcelos, T.C.R. Ferreira, E.R. Pereira-Filho, M.R.V. Lanza, J. Adv. Oxid. Technol. 18 (2015) 9–14.
[27] H. Bel Hadjltaief, P. Da Costa, P. Beaunier, M.E. Gálvez, M. Ben Zina, Appl. Clay Sci. 91–92 (2014) 46–54.
[28] N. Banić, B. Abramović, J. Krstić, D. Šojić, D. Lončarević, Z. Cherkezova-Zheleva, V. Guzsvány, Appl. Catal. B: Environ. 107 (2011) 363–371.
[29] M. Munoz, Z.M. de Pedro, N. Menendez, J.A. Casas, J.J. Rodriguez, Appl. Catal. B: Environ. 136–137 (2013) 218–224.
[30] T. Zhou, Y. Li, J. Ji, F.-S. Wong, X. Lu, Sep. Purif. Technol. 62 (2008) 551–558.
[31] N. Tantiwa, A. Kuntiya, P. Seesuriyachan, Chiang Mai J. Sci. 40 (2013) 60–69.
[32] E. Saputra, S. Muhammad, H. Sun, H.M. Ang, M.O. Tadé, S. Wang, Catal. Today 190 (2012) 68–72.
[33] A.A.S. Oliveira, I.F. Teixeira, T. Christofani, J.C. Tristão, I.R. Guimarães, F.C.C. Moura, Appl. Catal. B: Environ. 144 (2014) 144–151.
[34] A.A.S. Oliveira, D.A.S. Costa, I.F. Teixeira, F.C.C. Moura, Appl. Catal. B: Environ. 162 (2015) 475–482.
[35] R.C.C. Costa, F.C.C. Moura, P.E.F. Oliveira, F. Magalhães, J.D. Ardisson, R.M. Lago, Chemosphere 78 (2010) 1116–1120.
[36] Q. Chen, P. Wu, Y. Li, N. Zhu, Z. Dang, J. Hazard. Mater. 168 (2009) 901–908.
[37] Y. Mamindy-Pajany, B. Hamer, M. Roméo, F. Géret, F. Galgani, E. Durmiši, C. Hurel, N. Marmier, Chemosphere 82 (2011) 362–369.
[38] A.A.S. Oliveira, J.C. Tristao, J.D. Ardisson, A. Dias, R.M. Lago, Appl. Catal. B 105 (2011) 163–170.
[39] Y. Boyjoo, M. Ang, V. Pareek, Chem. Eng. Sci. 93 (2013) 11–21.
[40] C. Ruales-Lonfat, J.F. Barona, A. Sienkiewicz, M. Bensimon, J. Vélez-Colmenares, N. Benítez, C. Pulgarín, Appl. Catal. B: Environ. 166–167 (2015) 497–508.
[41] M. Vinita, R. Praveena Juliya Dorathi, K. Palanivelu, Solar Energy 84 (2010) 1613–1618.
[42] A. Safarzadeh-Amiri, J.R. Bolton, S.R. Cater, Adv. Oxid. Technol. 1 (1996) 18–26.
[43] J.J. Pignatello, E. Oliveros, A. MacKay, Crit. Rev. Environ. Sci. Technol. 36 (2006) 1–84.
[44] Y. Gao, H. Gan, G. Zhang, Y. Guo, Chem. Eng. J. 217 (2013) 221–230.
[45] O. Primo, M.J. Rivero, I. Ortiz, J. Hazard. Mater. 153 (2008) 834–842.
[46] M.Y. Ghaly, G. Härtel, R. Mayer, R. Haseneder, Waste Manag. 21 (2001) 41–47.
[47] R.F.B. Nogueira, A.G. Trovó, M.R.A. Silva, R.D. Villa, Quim. Nova 30 (2007) 400–408.
[48] F.F.S. Dias, R.J. Lira, O. Chiavone-Filho, F.O. Carvalho, J.G. Pacheco, Sci. Plena 9 (2013).
[49] D. Sannino, V. Vaiano, P. Ciambelli, L.A. Isupova, Chem. Eng. J. 224 (2013) 53–58.
[50] D. Monllor-Satoca, R. Gómez, M. González-Hidalgo, P. Salvador, Catal. Today 129 (2007) 247–255.
[51] R.A. Palominos, A. Mora, M.A. Mondaca, M. Pérez-Moya, H.D. Mansilla, J. Hazard. Mater. 158 (2008) 460–464.
[52] I.K. Konstantinou, T.A. Albanis, Appl. Catal. B: Environ. 49 (2004) 1–14.
[53] A. Karci, Chemosphere 99 (2014) 1–18.
[54] V. Kokkali, W. van Delft, TRAC Trends Anal. Chem. 61 (2014) 133–155.
[55] -.N. Safety data sheet. 1, https://www.fishersci.ca/viewmsds.do?catNo=AC166711000], 2015.
[56] V.M. Vasconcelos, F.L. Ribeiro, F.L. Migliorini, S.A. Alves, J.R. Steter, M.R. Baldan, N.G. Ferreira, M.R.V. Lanza, Electrochim. Acta 178 (2015) 484–493.
[57] R. Gonzalez-Olmos, F. Holzer, F.D. Kopinke, A. Georgi, Appl. Cata. A: Gen. 398 (2011) 44–53.
[58] S. Rahim Pouran, A.A. Abdul Raman, W.M.A. Wan Daud, J. Clean. Prod. 64 (2014) 24–35.
[59] Q. Wang, S. Tian, J. Long, P. Ning, Catal. Today 224 (2014) 41–48.
[60] F. Haber, J. Weiss, Proc. R. Soc. Lond. Ser. A—Math. Phys. Sci. 147 (1934) 332–351.
[61] R.C.C. Costa, F.C.C. Moura, J.D. Ardisson, J.D. Fabris, R.M. Lago, Appl. Catal. B: Environ. 83 (2008) 131–139.
[62] F.C.C. Moura, M.H. Araujo, R.C.C. Costa, J.D. Fabris, J.D. Ardisson, W.A.A. Macedo, R.M. Lago, Chemosphere 60 (2005) 1118–1123.
[63] A.D. Bokare, W. Choi, J. Hazard. Mater. 275 (2014) 121–135.
[64] P. Raizada, P. Singh, A. Kumar, B. Pare, S.B. Jonnalagadda, Sep. Purif. Technol. 133 (2014) 429–437.
[65] Y. Segura, F. Martínez, J.A. Melero, R. Molina, R. Chand, D.H. Bremner, Appl. Catal. B: Environ. 113–114 (2012) 100–106.
[66] C.C. Amorim, M.M.D. Leão, R.F.P.M. Moreira, J.D. Fabris, A.B. Henriques, Chem. Eng. J. 224 (2013) 59–66.